Automatic Tuning of Cascade PID Control Systems

with Application to Attitude Control of UAVs

Liuping Wang

School of Engineering
Royal Melbourne Institute of Technology University
Australia

Outline

Outline

System suitable for cascade control

- A typical system suitable for cascade control is shown in Figure 1.
- The variable between the transfer functions, $x_1(t)$, is measurable.

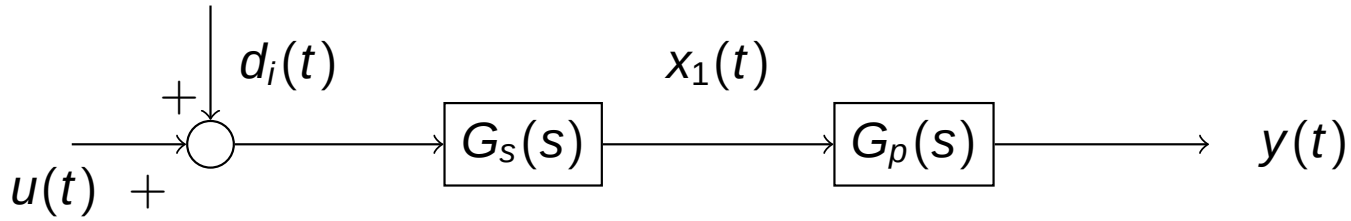

Figure 1: Block diagram for a system suitable for cascade control

Cascade control structure

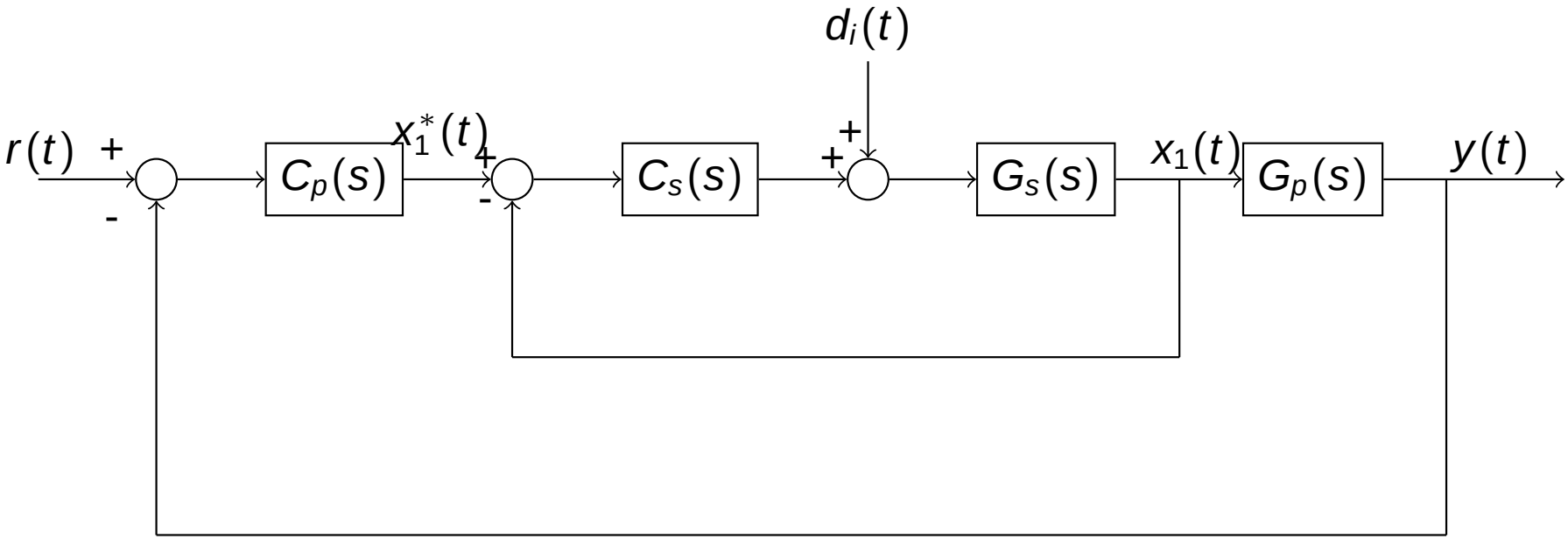

Figure 2: Block diagram of a cascade control system

Secondary and primary systems

The inner-loop system is the secondary system and the outer-loop system is the primary system. The link between these two loops is the reference signal $x_1^*(t)$.

Design Steps

Subsystems

A complex system is decomposed into a series of first order or second order subsystems based on the considerations of physical relationships and availability of measurements.

Subsystem controllers

Design P, PI, PID, PD for each of the subsystems depending on the requirements. In general, the outer- loop systems are required to contain integral action for eliminate steady-state errors.

Design procedures

In the design process, the inner-loop control system is designed first and the closed-loop transfer function for the inner-loop system is obtained. The outer-loop control system is designed based on the outer-loop system, where the relatively small time constants resulted from the inner closed- loop system are neglected, but its steady-state gain is taken into account in the outer-loop model.

Stability and Performance Analysis

- Robust stability and performance analysis are performed, and closed-loop performances are adjusted using the bandwidths of the inner-loop and outer-loop systems.
- This step is important because there are neglected dynamics in the cascade control system.
- In principle, the bandwidth of the inner closed-loop control should be much wider than the one used in the outer closed-loop control. Namely, the inner-loop control system should have a much faster response speed for obtaining the closed-loop stability of the cascade control system.
- In the implementation, a wider bandwidth for the secondary closed-loop system is desired and also achieved by putting proportional control K_c on the feedback error.

Design Example: PI +PI

$$G_s(s) = \frac{5}{s+10}; \quad G_p(s) = \frac{0.005}{s+0.05}$$

Design a cascade control system with two PI controllers. For simplicity, we select the damping coefficient $\xi = 0.707$ for both inner and outer-loop control systems and use the bandwidths w_{ns} and w_{np} as the tuning parameters of the inner (secondary) and outer-loop (primary) systems respectively.

Pole-assignment Controller Design

For the inner-loop control system, we choose $w_{ns} = 5 \times 10 = 50$ leading to a pair of closed-loop poles at $-35.35 \pm j35.3607$, and for the outer-loop system, we choose $w_{np} = 4 \times 0.05 = 0.2$ leading to a pair of closed-loop poles at $-0.1414 \pm j0.1414$. These selections give us the ratio of inner-loop bandwidth to outer-loop bandwidth of 250.

The inner-loop control system

Controller parameters

$$K_{cs} = \frac{2\xi w_{ns} - a}{b} = \frac{2\xi w_{ns} - 10}{5} = 12.14;$$
$$\tau_{Is} = \frac{2\xi w_{ns} - a}{w_{ns}^2} = \frac{2\xi w_{ns} - 10}{w_{ns}^2} = 0.0243$$

Closed-loop transfer function

The closed-loop transfer function between the reference signal $X_1^*(s)$ and the output signal $X_1(s)$ is calculated as

$$\frac{X_1(s)}{X_1^*(s)} = \frac{(2\xi w_{ns} - 10)s + w_{ns}^2}{s^2 + 2\xi w_{ns} s + w_{ns}^2} \quad (1)$$

The outer-loop control system

To design the outer-loop controller, we consider the transfer function between $X_1^*(s)$ and the output $Y(s)$, which is

$$\frac{Y(s)}{X_1^*(s)} = \frac{(2\xi w_{ns} - 10)s + w_{ns}^2}{s^2 + 2\xi w_{ns} s + w_{ns}^2} \frac{0.005}{s + 0.05} \tag{2}$$

We neglect the inner-closed-loop system by considering

$$\frac{X_1(s)}{X_1^*(s)} = \frac{\frac{(2\xi w_{ns} - 10)}{w_{ns}^2}s + 1}{\frac{1}{w_{ns}^2}s^2 + \frac{2\xi}{w_{ns}}s + 1} \approx 1 \tag{3}$$

$$K_{cp} = \frac{2\xi w_{np} - 0.05}{0.005} = 46.56; \quad \tau_{Ip} = \frac{2\xi w_{np} - 0.05}{w_{np}^2} = 5.82$$

where $w_{np} = 0.2$.

Closed-loop poles

- One can verify that there are four closed-loop poles with the following values: $-35.2335 \pm j35.4441$ and $-0.1415 + \pm j0.1415$.
- The pair of dominant closed-loop poles are almost equal to the performance specifications from the outer-loop control system and the remaining pair is close to the performance specification from the inner-loop control system.

Block Diagram for Cascade Control

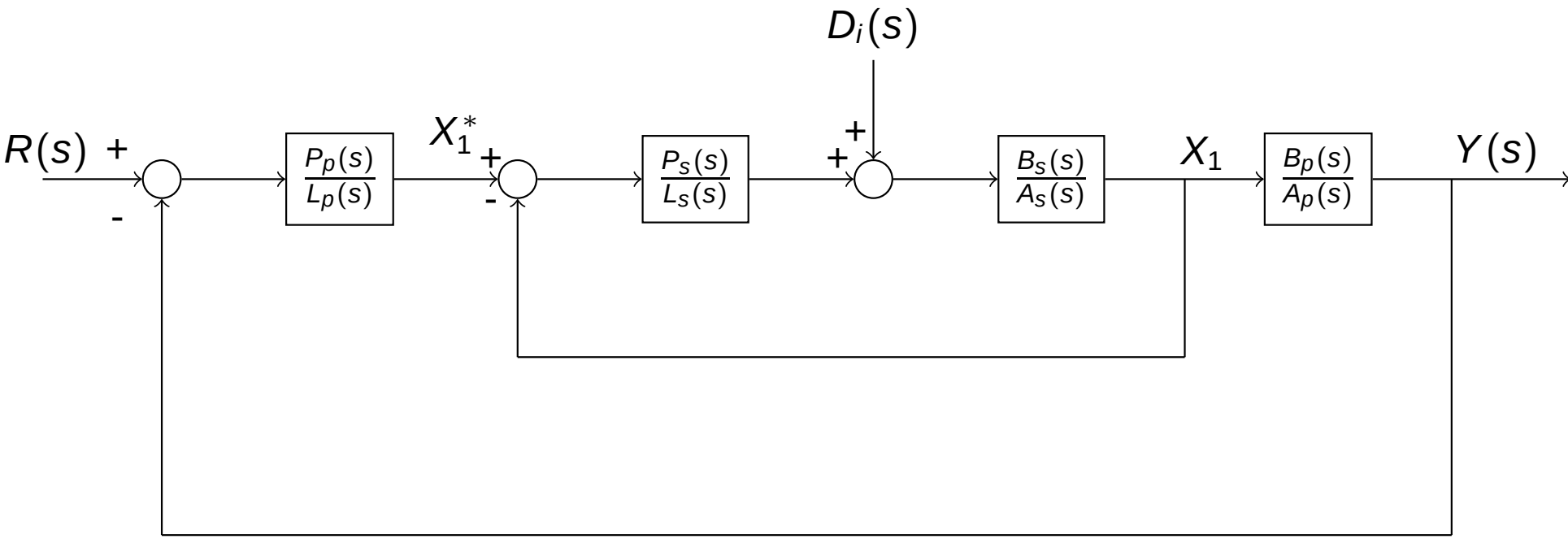

Figure 3: Closed-loop cascade control system

Closed-loop Transfer Function For Disturbance Rejection (i)

- To examine the effectiveness of disturbance rejection, we calculate the closed-loop transfer function between the disturbance $D_i(s)$ and the output $Y(s)$ as shown in Figure 3. Here, we assume the reference signal $R(s) = 0$.
-

$$X_1(s) = \overbrace{\frac{B_s(s)P_s(s)}{A_s(s)L_s(s) + B_s(s)P_s(s)}}^{T(s)_s} X_1(s)^* + \overbrace{\frac{B_s(s)L_s(s)}{A_s(s)L_s(s) + B_s(s)P_s(s)}}^{S_i(s)_s} D_i(s) \tag{4}$$

$$X_1(s) = T(s)_s X_1(s)^* + S_i(s)_s D_i(s) \tag{5}$$

Closed-loop Transfer Function For Disturbance Rejection (ii)

The primary output $Y(s)$ is expressed as

$$\begin{aligned} Y(s) &= \frac{B_p(s)}{A_p(s)} X_1(s) \\ &= \frac{B_p(s)}{A_p(s)} (T(s)_s X_1(s)^* + S_i(s)_s D_i(s)) \end{aligned} \tag{6}$$

With the control signal $X_1(s)^*$ generated from the primary controller as

$$X_1(s)^* = -\frac{P_p(s)}{L_p(s)} Y(s)$$

we obtain the closed-loop transfer function from the input disturbance $D_i(s)$ to the output $Y(s)$:

$$\frac{Y(s)}{D_i(s)} = \frac{G_p(s) S_i(s)_s}{1 + G_p(s) C_p(s) T(s)_s} \tag{7}$$

Example

Consider the position control of a DC motor in the presence of unknown load T_L. The relationship between the input voltage $V(s)$ and the angular velocity of the motor $\Omega(s)$ is described by the normalized Laplace transfer function:

$$\frac{\Omega(s)}{V(s)} = \frac{e^{-ds}}{s+1} \tag{8}$$

where a small time delay $d = 0.0016$ (sec) is used to model the delay induced by the sensing and actuation devices. The angular position $\Theta(s)$ is related to the angular velocity through integration:

$$\frac{\Theta(s)}{\Omega(s)} = \frac{1}{s}$$

Design a cascade control system for the position control of the DC motor and show its advantage in terms of disturbance rejection of the unknown load.

Pole-assignment Controller Design

- For the cascade control system design, the secondary transfer function is

$$G_s(s) = \frac{e^{-ds}}{s+1}$$

- By neglecting the time delay, from the pole-assignment controller design, the proportional controller gain and the integral time constant are

$$K_{cs} = 2\xi w_{ns} - 1 = 34.35; \quad \tau_{Is} = \frac{2\xi w_{ns} - 1}{w_{ns}^2} = 0.0550$$

where $\xi = 0.707$ and $w_{ns} = 25$.

- The primary transfer function is

$$G_p(s) = \frac{1}{s}$$

and the proportional controller gain and the integral time constant are

$$K_{cp} = 2\xi w_{np} = 3.535; \quad \tau_{Ip} = \frac{2\xi}{w_{np}} = 0.5656$$

where $\xi = 0.707$ and $w_{np} = 2.5$

Sensitivity Analysis (i)

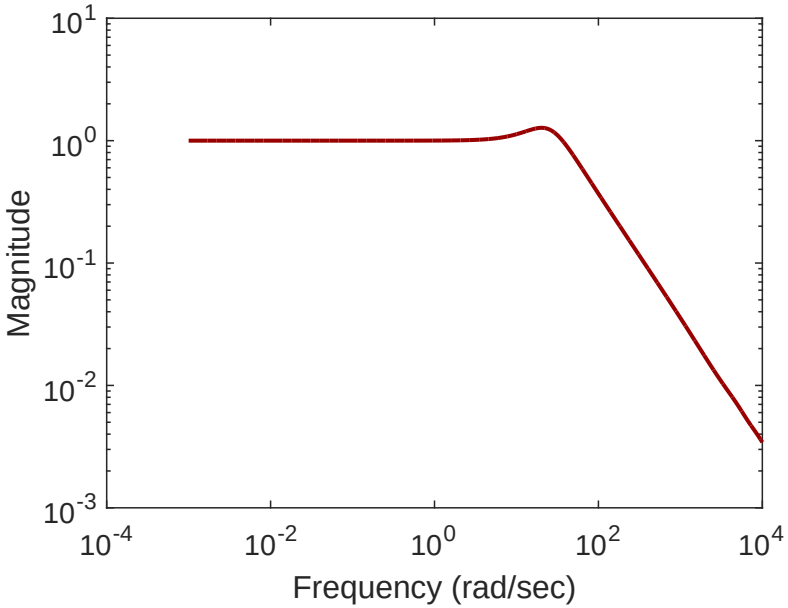

(a) Complementary sensitivity (secondary)

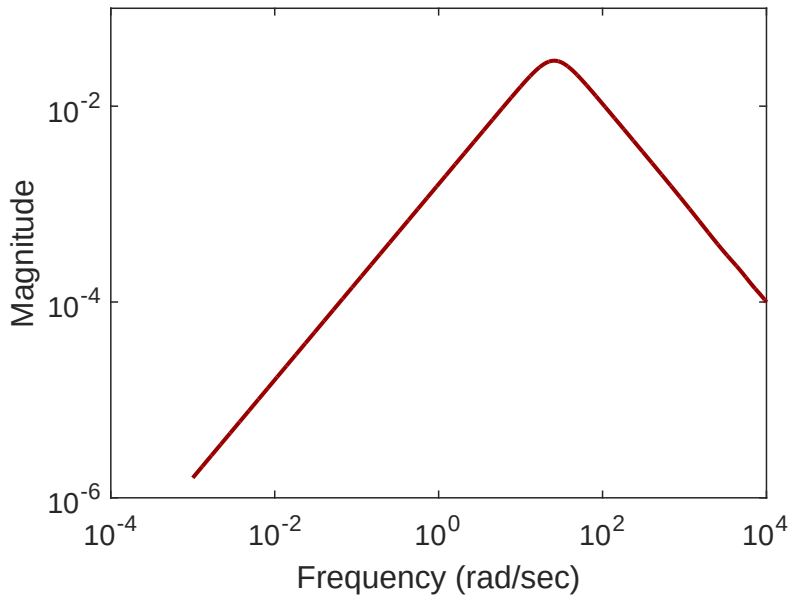

(b) Input sensitivity (secondary)

Figure 4: Sensitivity functions for the secondary control system

Sensitivity Analysis (ii)

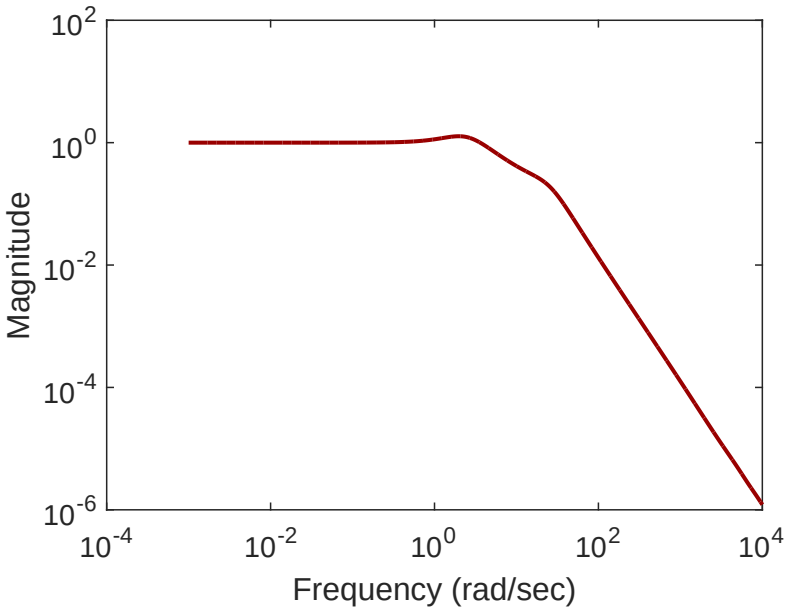

(a) Complementary sensitivity (primary)

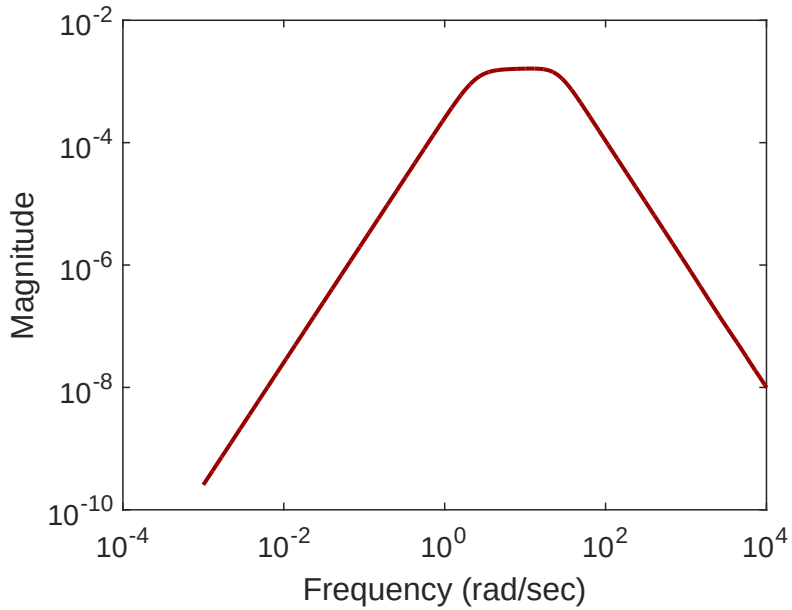

(b) Input sensitivity (primary)

Figure 5: Sensitivity functions for the cascade control system

Closed-loop Simulation Results

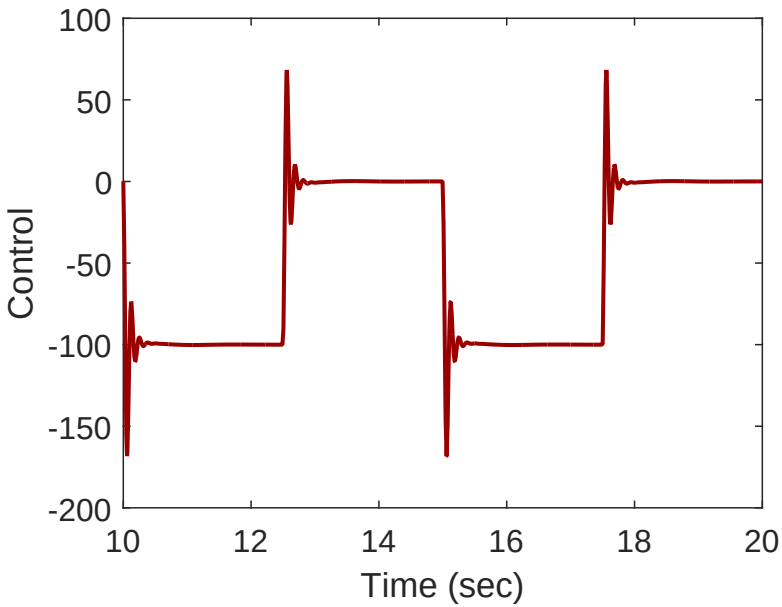

(a) Control signal

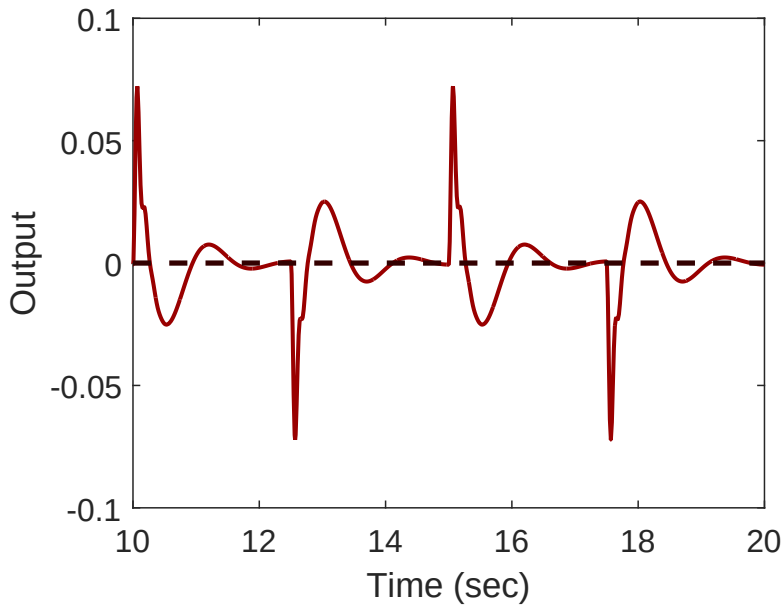

(b) Output signal

Figure 6: Cascade closed-loop response to square wave disturbance signal with amplitude 100 and period of 10.

Actuator with Deadzone

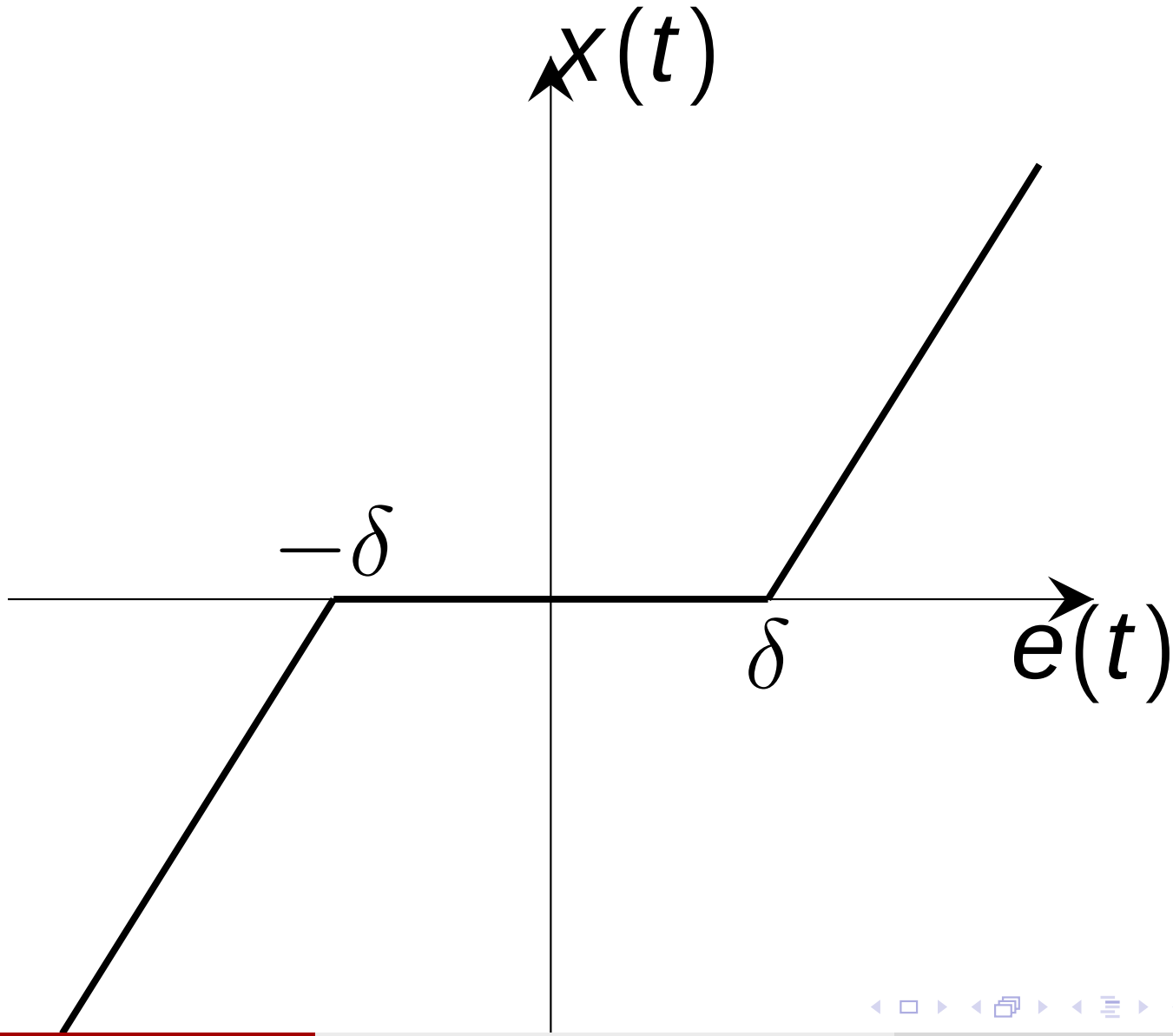

Deadzone Nonlinearity

Deadzone nonlinearity for an actuator, which is due to wearing and tearing, is described by the following equations:

$$x(t) = \begin{cases} e(t) - \delta & e(t) > \delta \\ 0 & -\delta \leq e(t) \leq \delta \\ e(t) + \delta & e(t) < \delta \end{cases} \tag{9}$$

Example

The actuator for a physical system is described by the transfer function

$$G_s(s) = \frac{0.5}{s + 15},$$

which is secondary plant. The primary plant is described by the transfer function:

$$G_p(s) = \frac{0.8}{(0.1s + 1)(s + 0.1)}. \tag{10}$$

There is a deadzone associated with the actuator.

Ignoring Actuator Dynamics

By neglecting this small time constant and taking consideration of the steady-state gain from the actuator, which is $\frac{0.5}{15}$, we obtain the approximate model for the PI controller design as

$$G(s) = \frac{0.5}{15}\frac{0.8}{s+0.1} = \frac{b}{s+a}$$

With $a = 0.1$, $b = 0.0267$, $w_n = 1$ and $\xi = 0.707$, we calculate the PI controller parameters as

$$K_c = \frac{2\xi w_n - a}{b} = 49.275; \quad \tau_I = \frac{2\xi w_n - a}{w_n^2} = 1.314.$$

Closed-loop Response

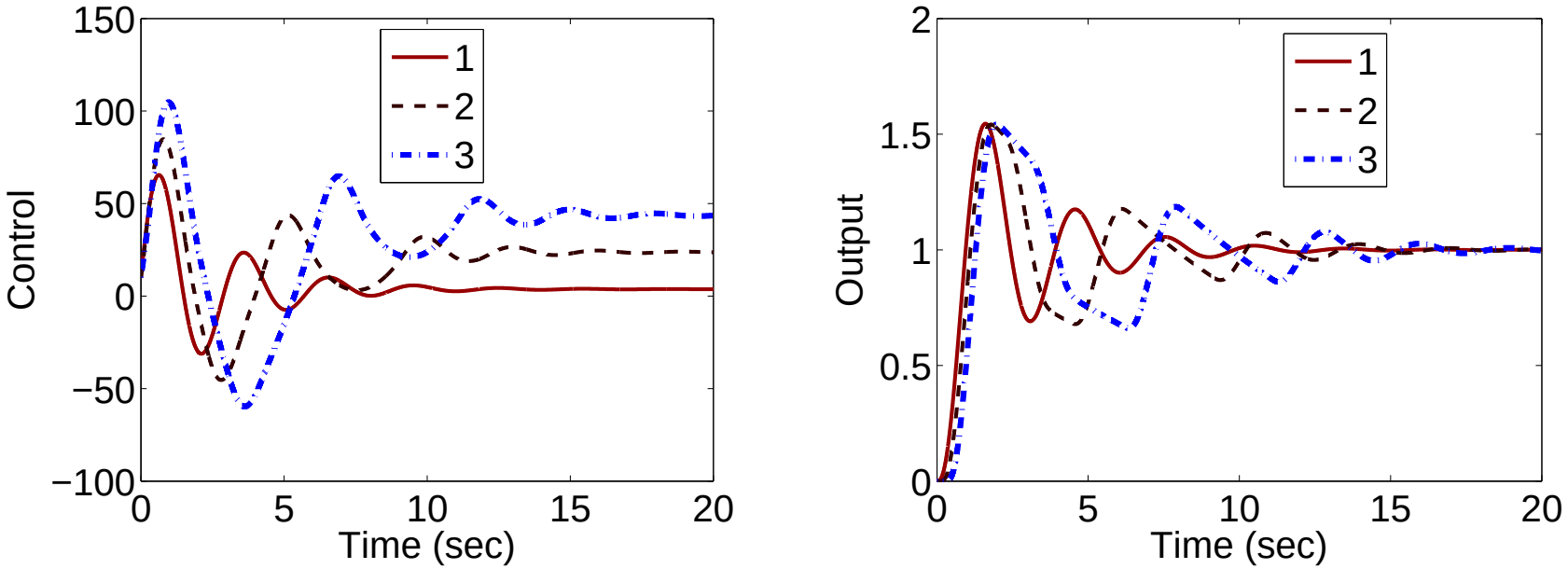

(a) Control signal (b) Output

Figure 8: Closed-loop control response by neglecting actuator dynamics. Key: line (1) response without deadzone; line (2) response with deadzone ($\delta = 20$); line (3) response with deazone ($\delta = 40$)

Cascade Control

We continue from this example. Instead of neglecting the actuator dynamics, we use a PI controller to control the actuator and a PI controller for the primary plant.

Inner-loop control

We select the natural frequency for the secondary control system as $w_{ns} = 20$, which is 20 times of that used for the primary control system. With this selection, the PI controller parameters are

$$K_{cs} = \frac{2 \times 0.707 \times 20 - 15}{0.5} = 26.56; \tau_{Is} = \frac{2 \times 0.707 \times 20 - 15}{400} = 0.0332$$

Outer-loop control

In the design of primary controller, the inner-loop dynamics are neglected. Therefore, the PI controller is designed using the transfer function (10) for the primary plant, leading to

$$K_{cp} = \frac{2 \times 0.707 \times 1 - 0.1}{0.8} = 1.6425; \tau_{Ip} = \frac{2 \times 0.707 \times 1 - 0.1}{1} = 1.314.$$

Simulation Program

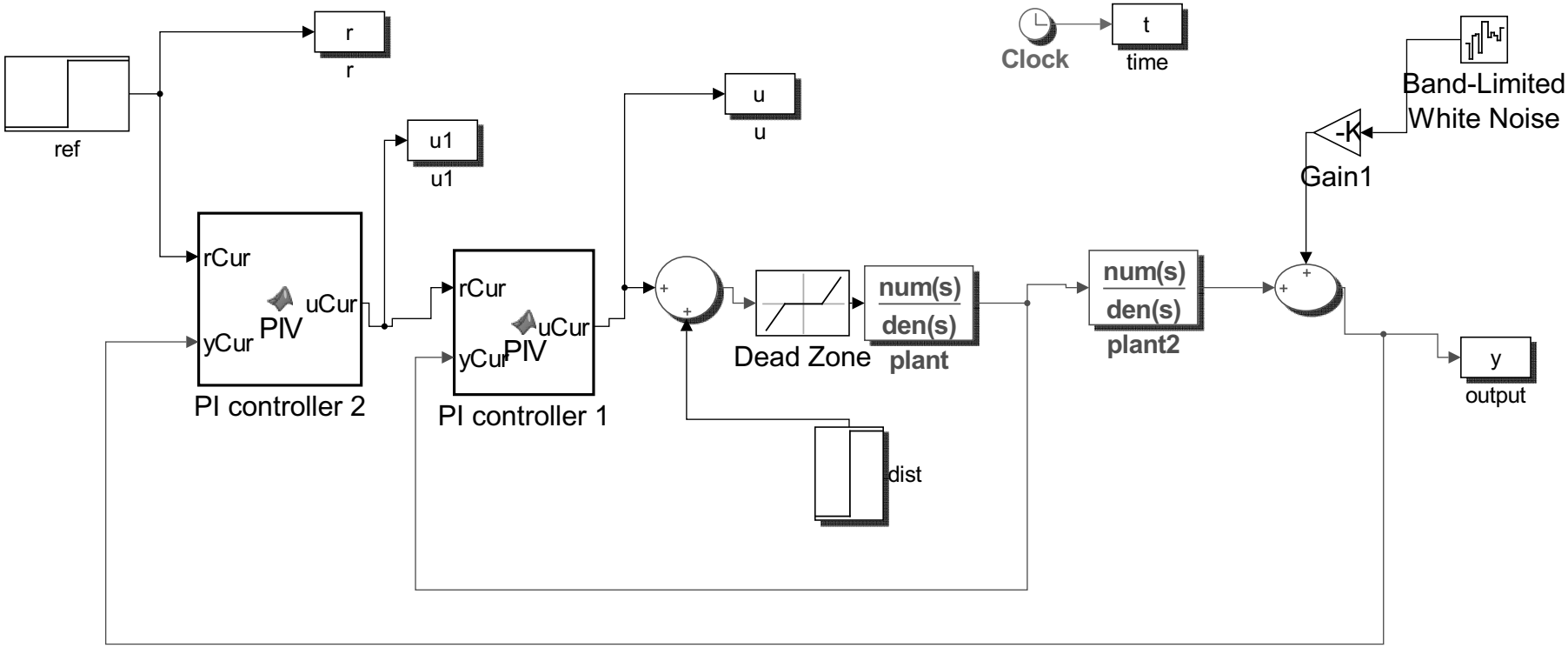

Figure 9: Simulink simulation program for the cascade control system with deadzone nonlinearity in the actuator.

Simulation Results

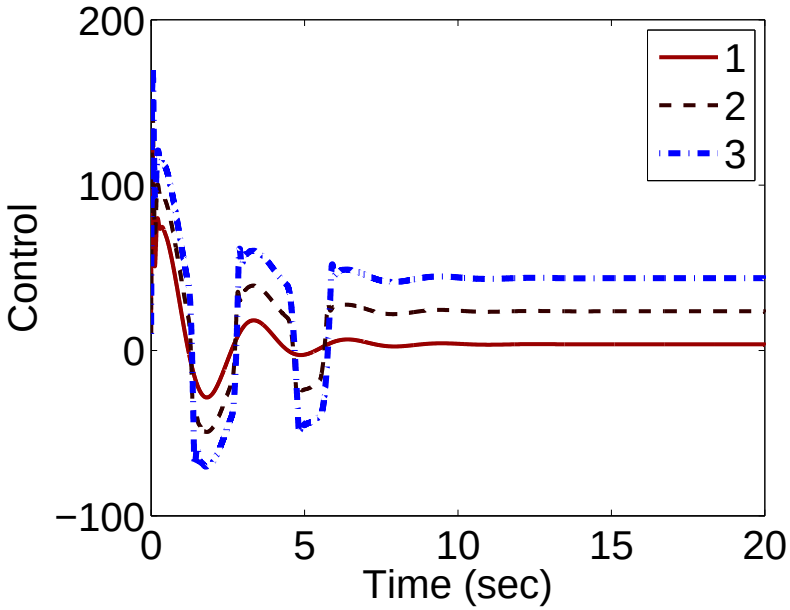

(a) Control signal

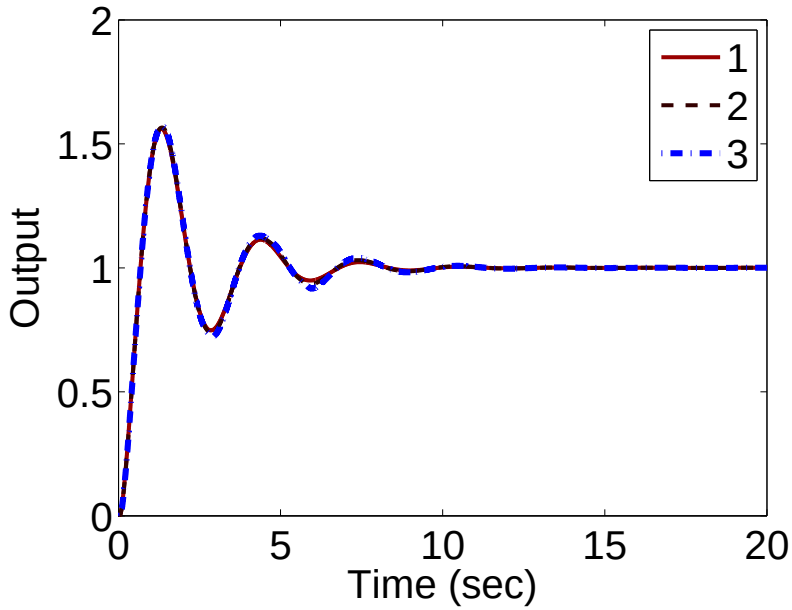

(b) Output

Figure 10: Closed-loop control response using cascade control ($w_{ns} = 20$, $w_{np} = 1$). Key: line (1) response without deadzone; line (2) response with deadzone ($\delta = 20$); line (3) response with deadzone ($\delta = 40$)

Outline

Multi-rotor UAVs

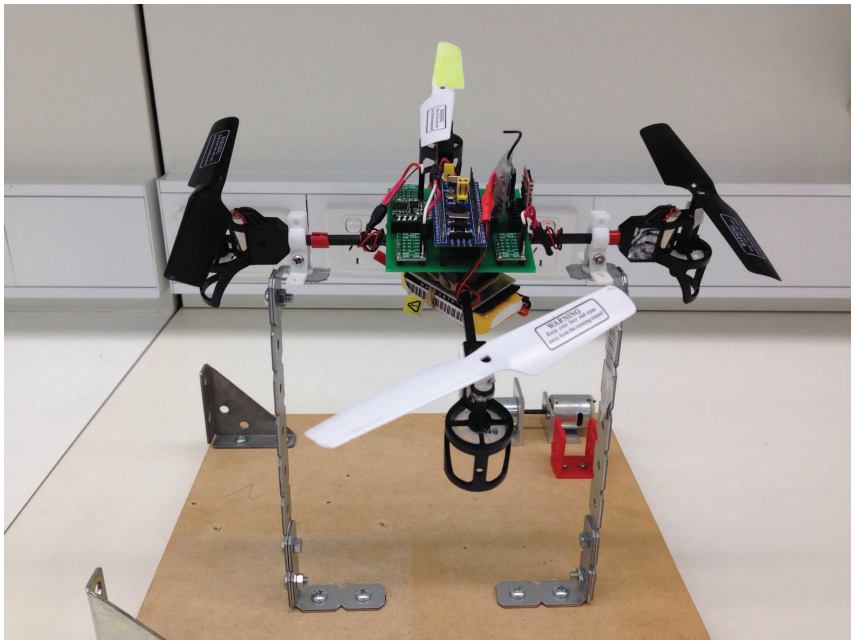

(a) Quadrotor

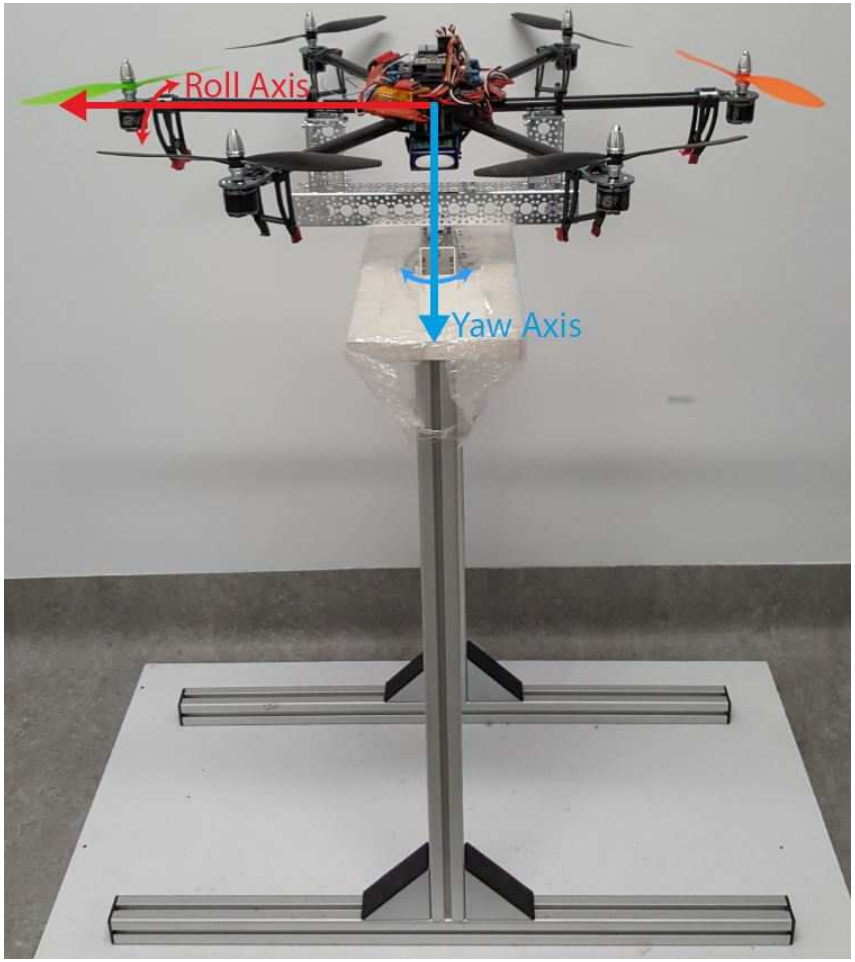

(b) Hexacopter

Figure 11: Unmanned aerial vehicles (multi-rotor)

Dynamic Model

Model

$$\begin{bmatrix} \dot{p} \\ \dot{q} \\ \dot{r} \end{bmatrix} = \begin{bmatrix} (I_{yy} - I_{zz})qr/I_{xx} \\ (I_{zz} - I_{xx})pr/I_{yy} \\ (I_{xx} - I_{yy})pq/I_{zz} \end{bmatrix} + \begin{bmatrix} 1/I_{xx} & 0 & 0 \\ 0 & 1/I_{yy} & 0 \\ 0 & 0 & 1/I_{zz} \end{bmatrix} \begin{bmatrix} \tau_x \\ \tau_y \\ \tau_z \end{bmatrix} \quad (11)$$

Parameters

I_{xx}, I_{yy} and I_{zz} are the moments of inertia for the three axes in x, y, z directions; p, q and r the body frame angular velocities in x, y, z directions; τ_x, τ_y, τ_z are the corresponding torques in x, y, z directions. The multi-rotor is assumed to have symmetric structure.

Relationships between ϕ, θ, ψ and p, q, r

Roll, pitch and yaw

The attitude of a multi-rotor is captured by the variations of the three Euler angles: roll angle ϕ, pitch angle θ and yaw angle ψ. The roll angle ϕ is to define the rotation about the x body axis, pitch angle θ is about y body axis, and yaw angle is about z body axis.

The relationship

$$\begin{bmatrix} \dot{\phi} \\ \dot{\theta} \\ \dot{\psi} \end{bmatrix} = \begin{bmatrix} 1 & \sin(\phi)\tan(\theta) & \cos(\phi)\tan(\theta) \\ 0 & cos(\phi) & -sin(\phi) \\ 0 & sin(\phi)/\cos(\theta) & \cos(\phi)/cos(\theta) \end{bmatrix} \begin{bmatrix} p \\ q \\ r \end{bmatrix}. \tag{12}$$

Attitude Control (i)

System Outputs

- For attitude control of quadrotor, the objective is to feedback control the three Euler angles so that they follow three reference signals (ϕ^*, θ^*, ψ^*).
- Therefore, the outputs of the control systems are the three Euler angles: ϕ, θ, ψ.

Control variables or manipulated variables

The manipulated variables or the control signals are the three torques, τ_x, τ_y, τ_z, along the x, y and z directions.

Attitude Control (ii)

Intermittent variables

The body frame angular velocities p, q and r along the x, y and z directions are the intermittent variables.

Cascade control

- Because there are two sets of nonlinear dynamic equations, cascade control is a good choice for this nonlinear control problem.
- The body frame angular velocities p, q and r are the secondary variables because they are directly related to the manipulated variables τ_x, τ_y and τ_z.
- The three Euler angles, ϕ, θ, ψ are the primary variables to achieve the attitude control

Cascade Control of One Axis

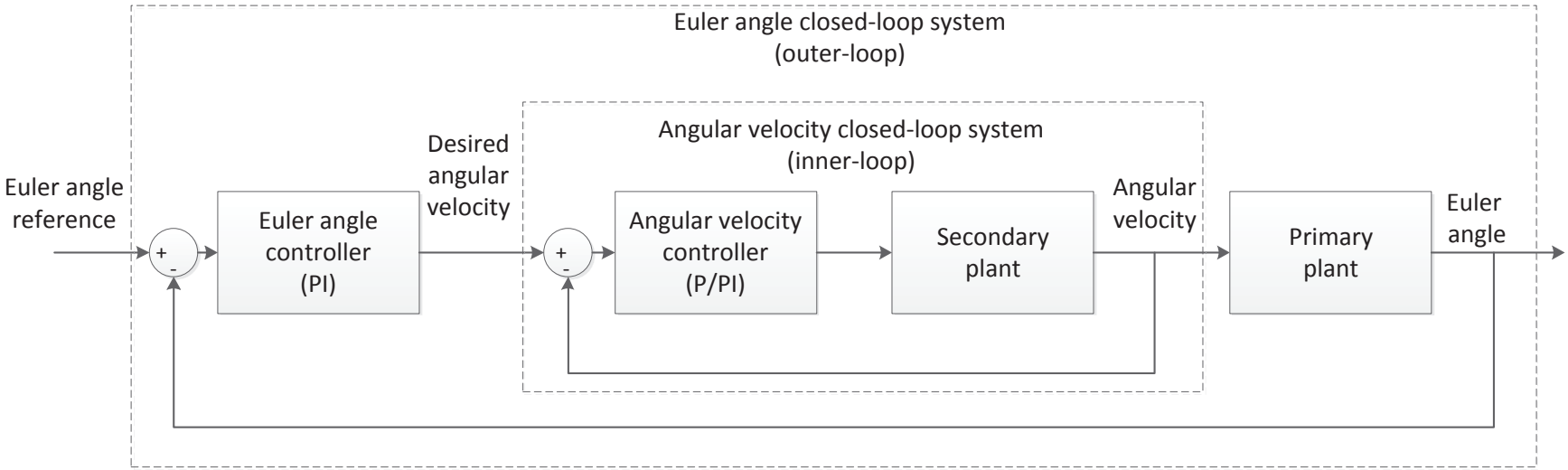

Figure 12: Cascade feedback control structure

Discussions of Cascade Control

- The dynamics of three axes are almost decoupled, thus PI controllers are designed for each axis separately.
- The inner-loop controller (also called secondary controller) is to control inner-loop (secondary) plant, where its reference signal is the desired angular velocity that is also the control signal generated from the outer-loop (primary) controller.
- For the cascade control system, the primary objective is to control the outer-loop (primary) plant to achieve desired closed-loop performance.

Outline

Overview

Auto-tuning procedure

The inner-loop closed-loop system dynamics are considered when tuning outer-loop controller;

- Automatic tuning the inner-loop PID controller;
- Closed-loop control of the inner-loop system with the PID controller found;
- Automatic tuning of the outer-loop PID controller with the inner-loop closed;

UAV application

Both inner-loop and outer-loop systems are modelled using integrator plus delay.

Auto-tuner Mechanism for Integrating Systems

Relay Feedback Control

- A proportional controller with known gain K_T is used to stabilize the integrating system;
- a relay feedback control system is deployed for the output of the closed-loop system.

Block diagram

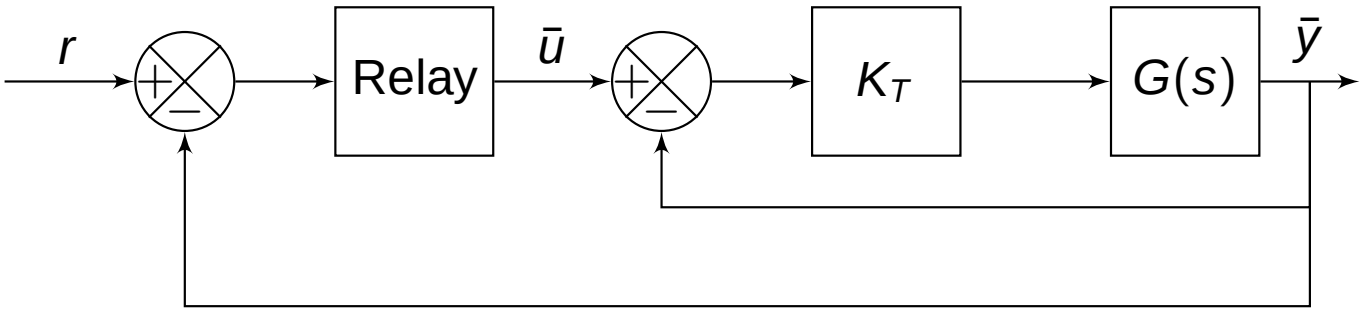

Figure 13: Relay feedback control system

The Input and Output Signals

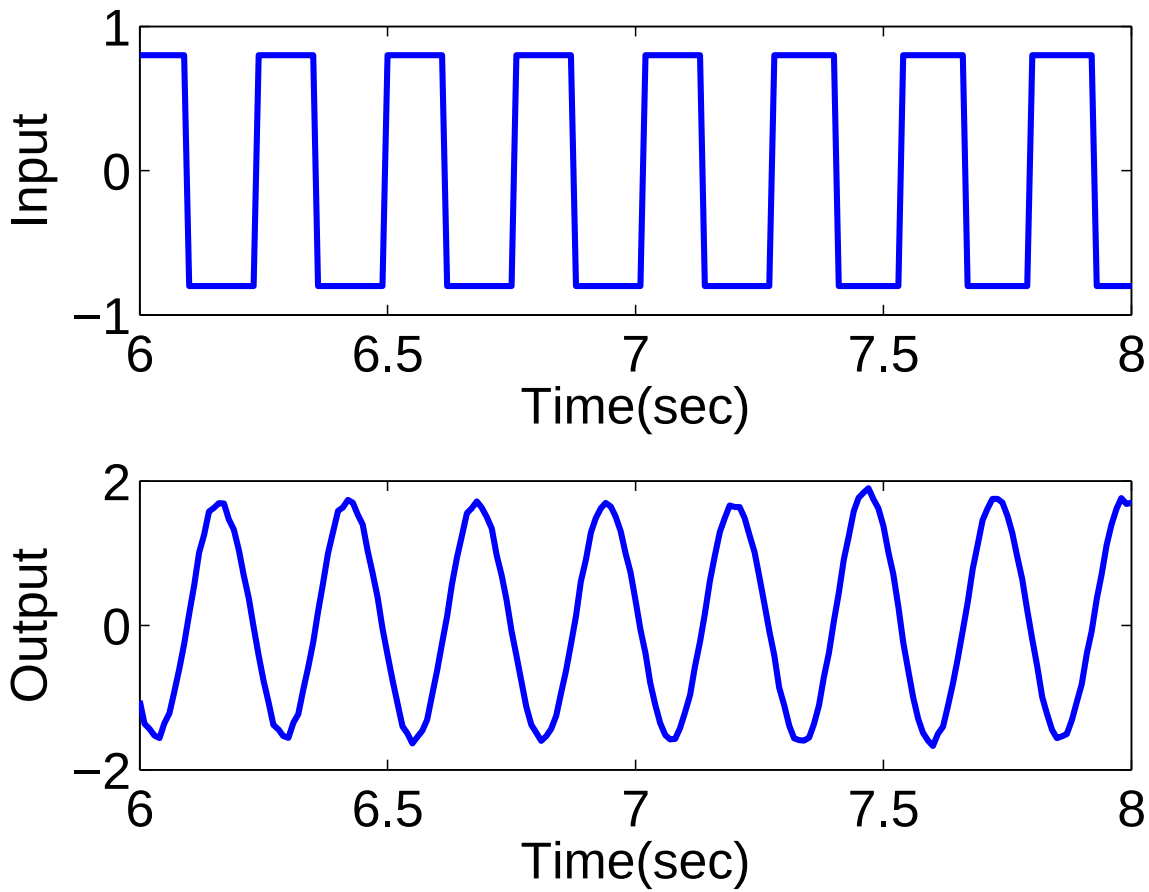

Figure 14: Relay feedback control signals: top figure input signal; bottom figure output signal.

Relay Control

- Calculate the relay feedback error: $e(t_k) = r(t_k) - \bar{y}(t_k)$.
- If $|e(t_k)| \leq \epsilon$; then $\bar{u}(t_k) = \bar{u}(t_{k-1})$.
- If $|e(t_k)| > \epsilon$; then $\bar{u}(t_k) = u_{ss} + a \times sign(e(t_k))$.
- u_{ss} is the steady-state value of input signal chosen to produce symmetric oscillation.

Notations

- The reference signal $r(t)$ is a constant that represents the steady-state operation of the plant.
- ϵ is the hysteresis selected to avoid the possible random switches caused by the measurement noise and a is the amplitude of the relay.
- The signal $\bar{y}(t)$ represents the actual output measurement.

The Characteristics of Relay Control

- Assume that the period of the oscillation is T.
- The frequency of the periodic signal $\bar{u}(t)$, denoting by $\omega_1 = \frac{2\pi}{T}$, approximately corresponds to the frequency illustrated on the Nyquist curve shown in Figure 15.

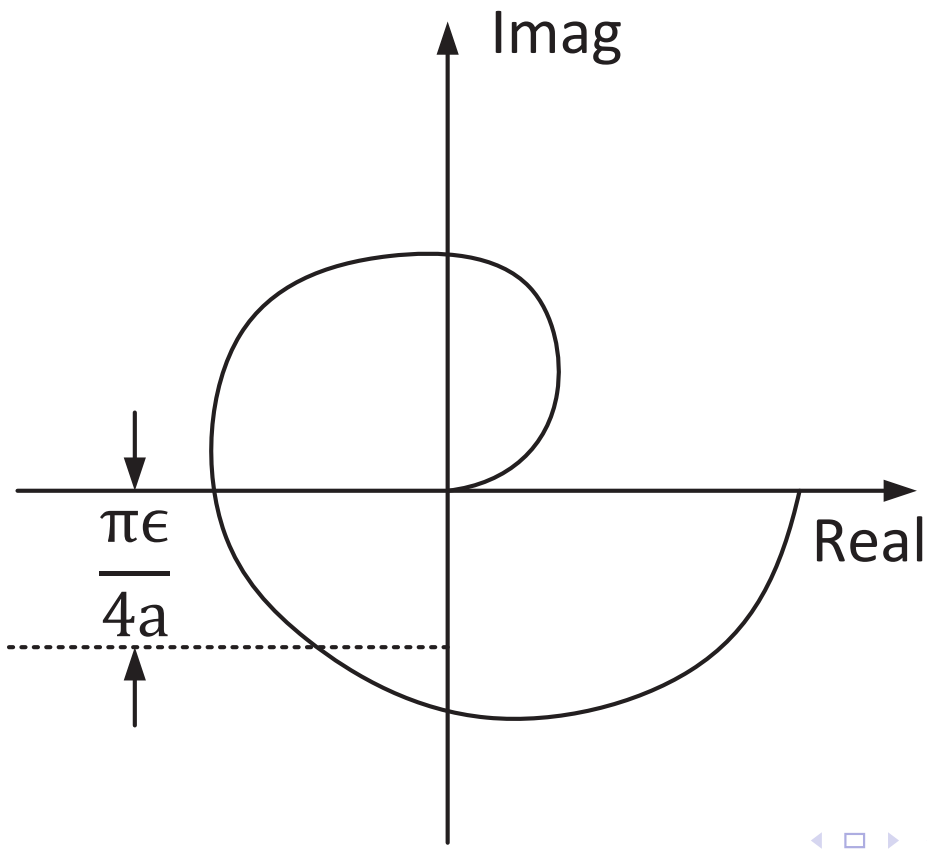

Estimation of Open-loop Frequency Response

To estimate the open-loop frequency response, the first step is to estimate the closed-loop frequency response

$$T(j\omega_1) = \frac{K_T G(j\omega_1)}{1 + K_T G(j\omega_1)}$$

where $G(j\omega_1)$ is the open-loop frequency response at ω_1.

Estimation of $T(j\omega_1)$

- The pair of input and output signals corresponding to the relay feedback control system is used.
- The input signal equals the relay output signal:

$$u(t) = \bar{u}(t) - u_{ss} = a \times sign(e(t))$$

- The closed-loop output signal with steady-state removed becomes

$$y(t) = \bar{y}(t) - r(t) = -e(t)$$

Characteristics of Periodic Signals

- For a period T, the Fourier series expansion of the periodic input signal $u(t)$, is expressed as

$$u(t) = \frac{4a}{\pi}(\sin\frac{2\pi}{T}t + \frac{1}{3}\sin\frac{6\pi}{T}t + \frac{1}{5}\sin\frac{10\pi}{T}t + \ldots) \tag{13}$$

- The fundamental frequency in continuous-time is $\frac{2\pi}{T}$.
- By choosing sampling interval Δt and the number of samples within one period $N = \frac{T}{\Delta t}$, the discretized input signal $u(t)$ at sampling instant $t_k = k\Delta t$ becomes

$$u(k) = \frac{4a}{\pi}(\sin\frac{2\pi k}{N} + \frac{1}{3}\sin\frac{6\pi k}{N} + \frac{1}{5}\sin\frac{10\pi k}{N} + \ldots) \tag{14}$$

- The fundamental frequency in discrete-time is $\frac{2\pi}{N}$.

Estimation of $T(j\omega_1)$ using Fast Fourier Transform

- The simplest way to estimate the frequency response of the system under relay feedback is to use Fast Fourier Transform.
- Assuming that the data length is L, the Fourier transform of the input signal $u(k)$, $k = 1, 2, \ldots, L$, is

$$U(n) = \frac{1}{L}\sum_{k=1}^{L} u(k)e^{-j\frac{2\pi(k-1)(n-1)}{L}} \tag{15}$$

and the corresponding Fourier transform of the output is

$$Y(n) = \frac{1}{L}\sum_{k=1}^{L} y(k)e^{-j\frac{2\pi(k-1)(n-1)}{L}} \tag{16}$$

where $n = 1,\ 2,\ 3,\ \ldots,\ L$.

- From both (15) and (16), with the definition of Fourier transform, the corresponding discrete frequency ω_d is defined from 0 to $\frac{2\pi(L-1)}{L}$ with an incremental of $\frac{2\pi}{L}$.

Example: Input and Output Data

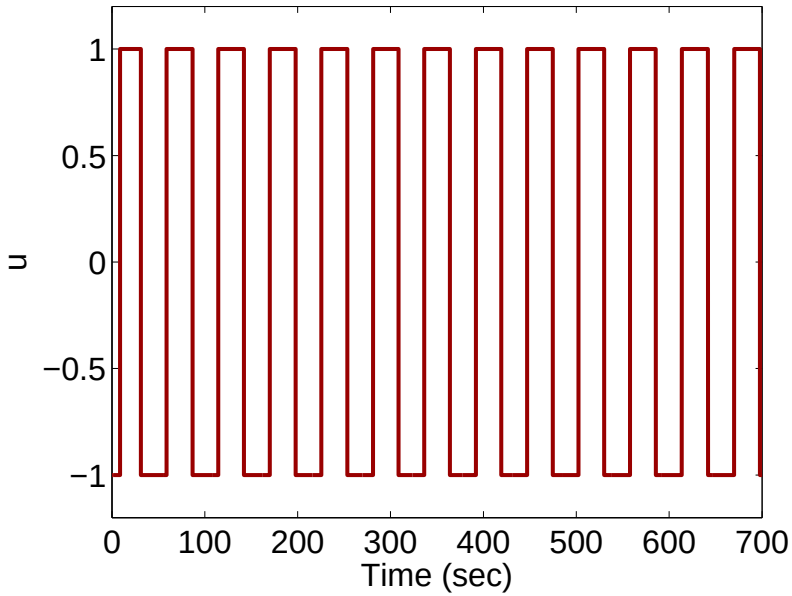

(a) Input data

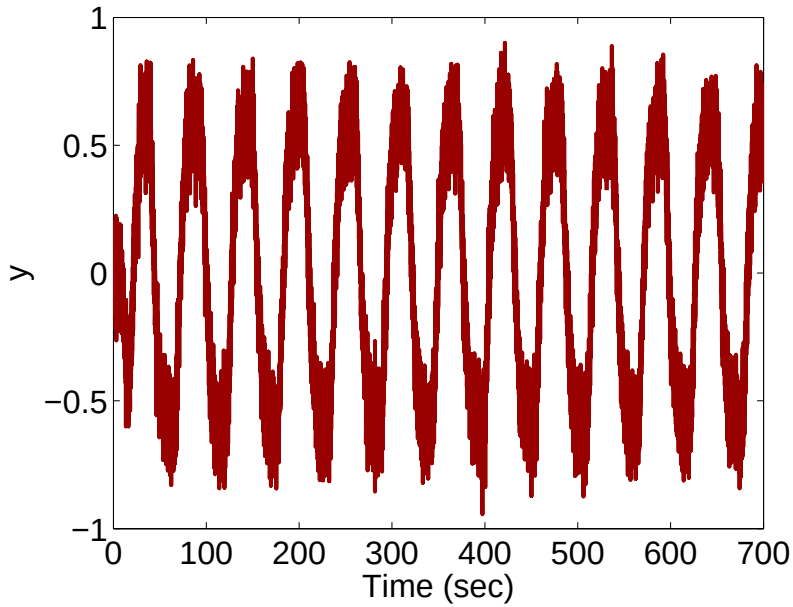

(b) Output data

Fourier Transform (1)

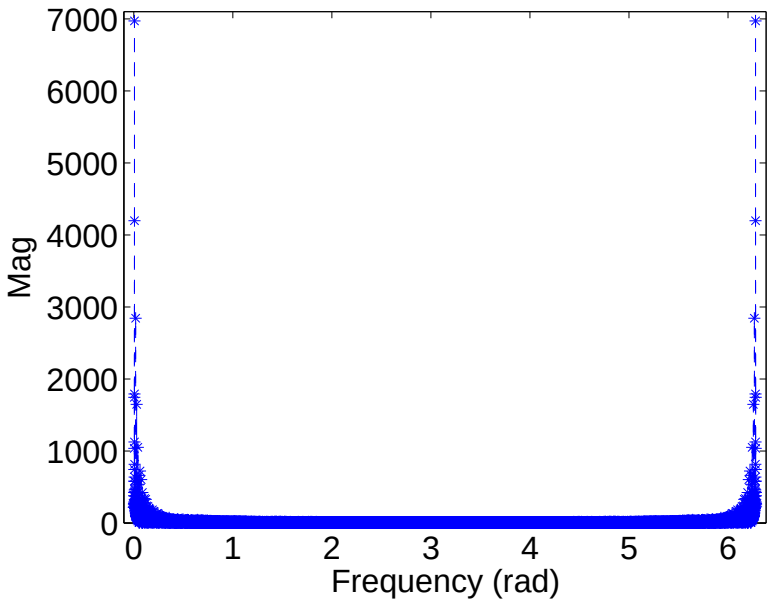

(c) Fourier transform $U(e^{j\omega_d})$

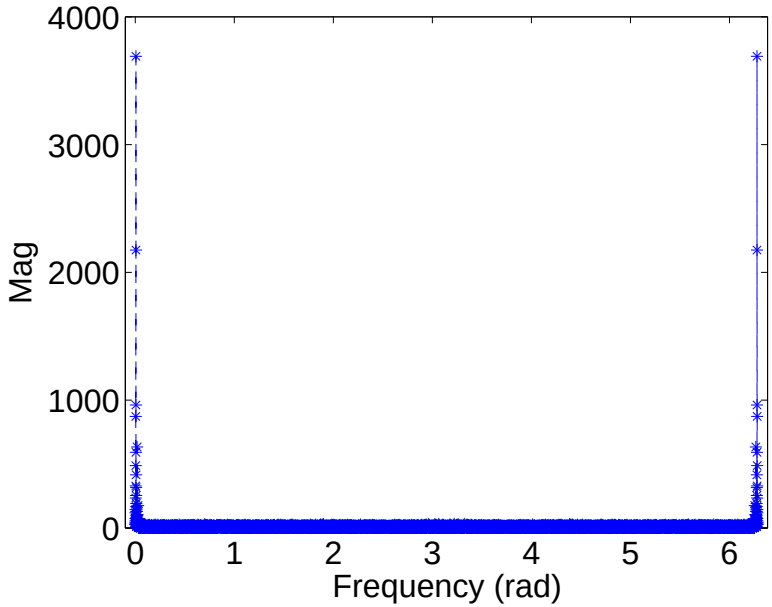

(d) Fourier transform $Y(e^{j\omega_d})$

Fourier Transform (2)

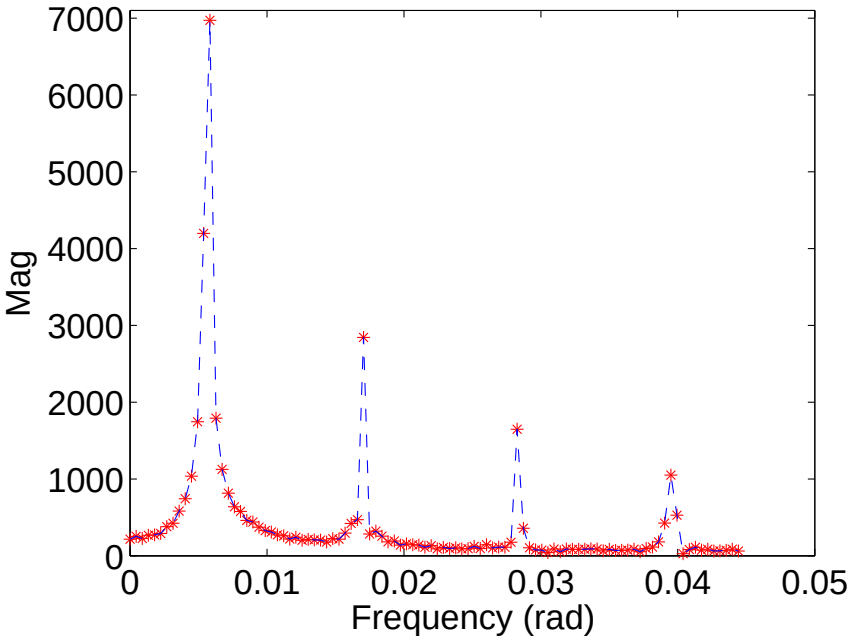

(e) Fourier transform $U(e^{j\omega_d})$, $0 \leq \omega_d \leq 0.045$

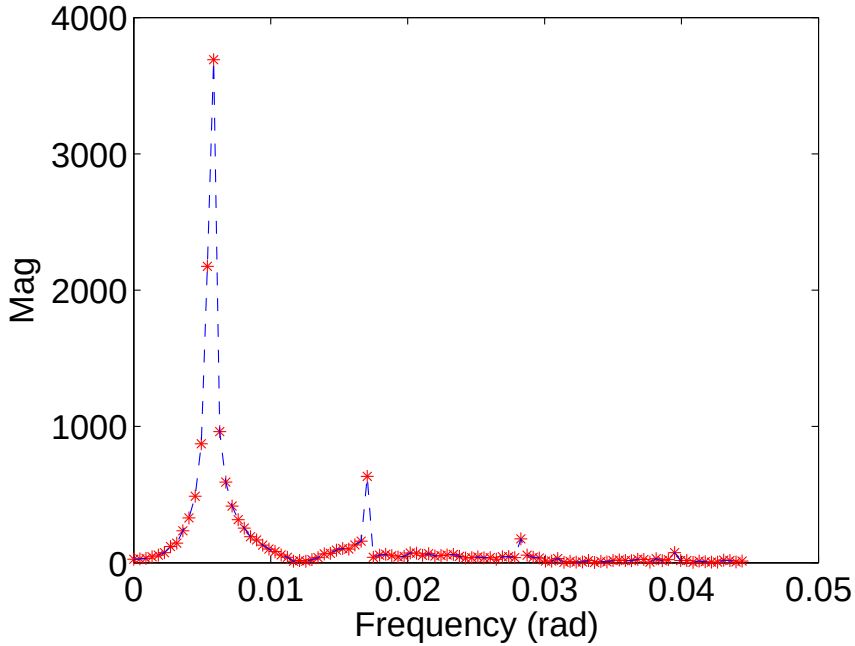

(f) Fourier transform $Y(e^{j\omega_d})$, $0 \leq \omega_d \leq 0.045$

Example (iii)

- Locating the fundamental frequency of the relay signal as the maximum value of $U(e^{j\omega_d})$, Identify the peaks of $U(e^{j\omega_d})$ as the $14th$ sample, which is the frequency at $\omega_d = \frac{2*\pi(14-1)}{L}$, $L = 14001$.
- The estimation of the frequency response of the system is then given by

$$T(14) = Y(14)/U(14) = -0.0040 - 0.5293i$$

- The second peak is identified at the $39th$ sample, which is the frequency at $\omega_d = \frac{2*\pi(39-1)}{L}$, $T = -0.1081 + 0.1950i$. The third peak is identified at $64th$ sample, which is the frequency at $\omega_d = \frac{2*\pi(64-1)}{L}$, $T = 0.1054 - 0.0151i$.
- Conversion between the frequencies: frequency in continuous-time ω_c equals $\omega_d/\Delta t$, where Δt is the sampling interval.

Integrator Plus Time Delay Model

- For an integrating plus time delay system, a single frequency is sufficient to determine its gain K_p and time delay d.
- The approximate model of an integrating system is assumed to be of the following form:

$$G_p(s) = \frac{K_p e^{-ds}}{s} \tag{17}$$

Finding the Parameters (i)

- Letting the frequency response of the integrator plus delay model (17) be equal to the estimated $G_p(j\omega_1)$ leads to

$$\frac{K_p e^{-jd\omega_1}}{j\omega_1} = G_p(j\omega_1) \tag{18}$$

- Equating the magnitudes on both side of (18) gives

$$K_p = \omega_1 |G_p(j\omega_1)| \tag{19}$$

where $|e^{-jd\omega_1}| = 1$.

Finding the Parameters (ii)

- Additionally, from (18), the following relationship holds:

$$e^{-jd\omega_1} = \frac{j\omega_1 G_p(j\omega_1)}{K_p}$$

- This gives the estimate of time delay as

$$d = -\frac{1}{\omega_1} tan^{-1} \frac{Imag(jG_p(j\omega_1))}{Real(jG_p(j\omega_1))} \tag{20}$$

PID Controller Design

The parameter β is the scaling factor for the desired closed-loop time constant, which is defined as

$$\tau_{cl} = \beta d$$

$$K_c = \frac{\hat{K}_c}{dK_p}$$

$$\tau_I = d\hat{\tau}_I$$

$$\tau_D = d\hat{\tau}_D$$

Normalized PID Parameters (i)

Table 1: Normalized PID controller parameters ($\xi = 0.707$)

	$0.7 \leq \beta \leq 1$	$1 < \beta \leq 11$
$\hat{K}_c$	$\frac{1}{0.3280\beta^2+0.0786\beta+0.6442}$	$\frac{1}{0.7184\beta+0.3661}$
$\hat{\tau}_I$	$-3.7845\beta^2 + 10.2044\beta - 4.0298$	$1.3970\beta + 1.2271$
$\hat{\tau}_D$	$\frac{1}{-1.9064\beta^2+6.1545\beta-1.5875}$	$\frac{1}{1.4275\beta+1.6450}$

Normalized PID Parameters (ii)

Table 2: Normalized PID controller parameters ($\xi = 1$)

	$0.7 \le \beta \le 1$	$1 < \beta \le 11$
$\hat{K}_c$	$\frac{1}{0.3100\beta^2 - 0.0486\beta + 0.7853}$	$\frac{1}{0.5138\beta + 0.5909}$
$\hat{\tau}_I$	$-3.0205\beta^2 + 9.6838\beta - 3.8821$	$1.9886\beta + 1.2118$
$\hat{\tau}_D$	$\frac{1}{-1.7078\beta^2 + 5.1844\beta - 1.0555}$	$\frac{1}{1.0156\beta + 1.7550}$

Outline

Application to Quadrotor

Function	Model
DC motor drive	DRV8833 Dual Motor Driver Carrier
Sensor board	MPU6050
Micro processor	STM32F103C8T6
RC receiver	WFLY065
DC motor	820 Coreless Motor
RC transmitter	WFT06X-A
Data logger	SparkFun OpenLog

Table 3: quadrotor hardware list

Experimental Data

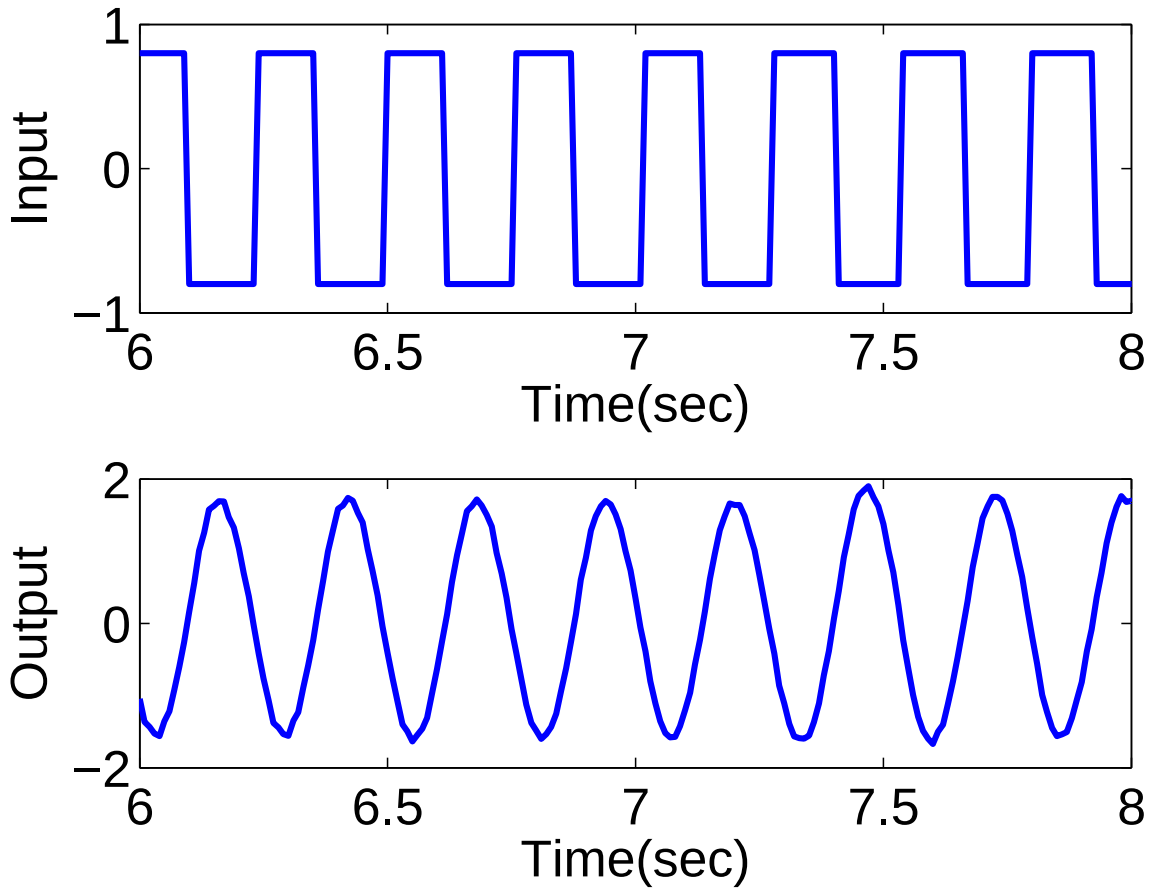

Figure 16: Relay feedback control signals from inner-loop system: top figure input signal; bottom figure output signal.

Closed-loop Control Results

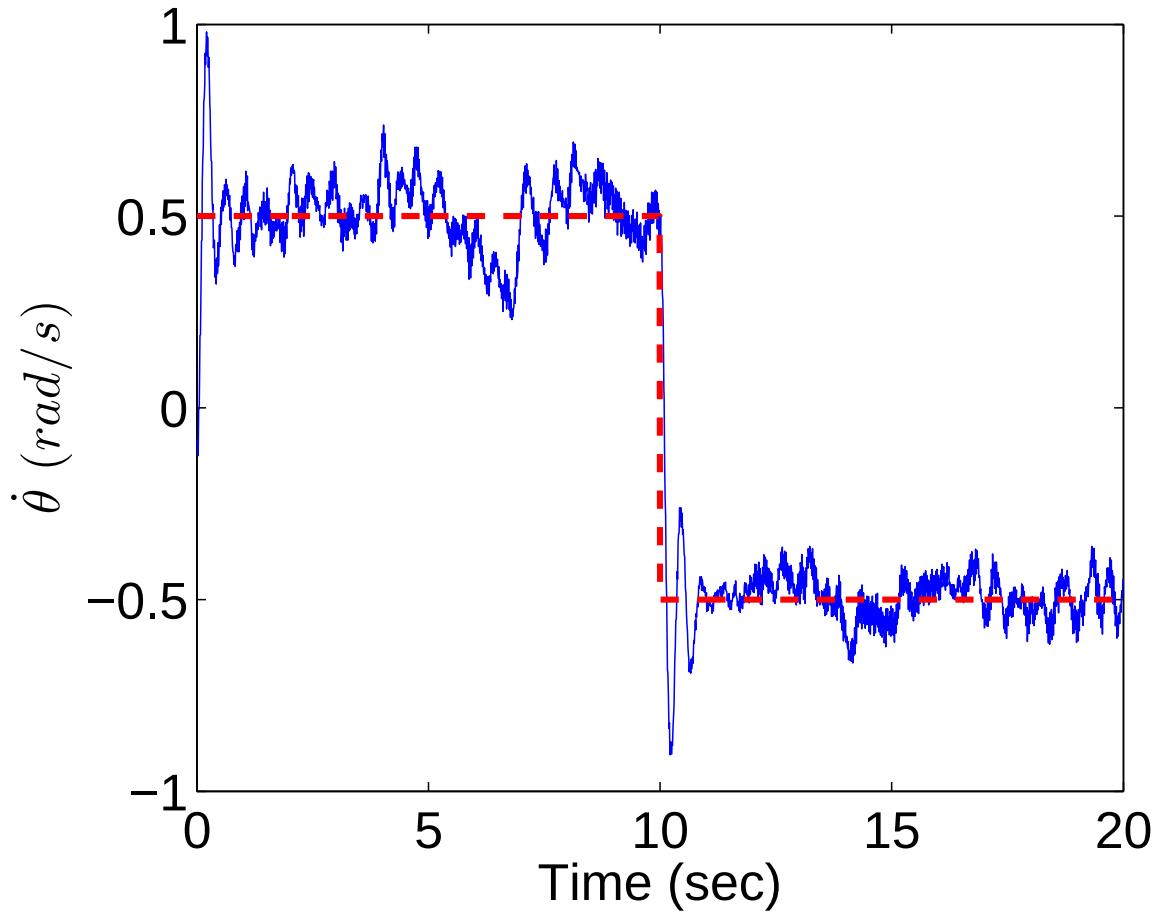

Figure 17: Inner-loop step response in closed-loop control. Dashed line: reference signal; solid line: output.

Auto-tuning of Primary PI Controller

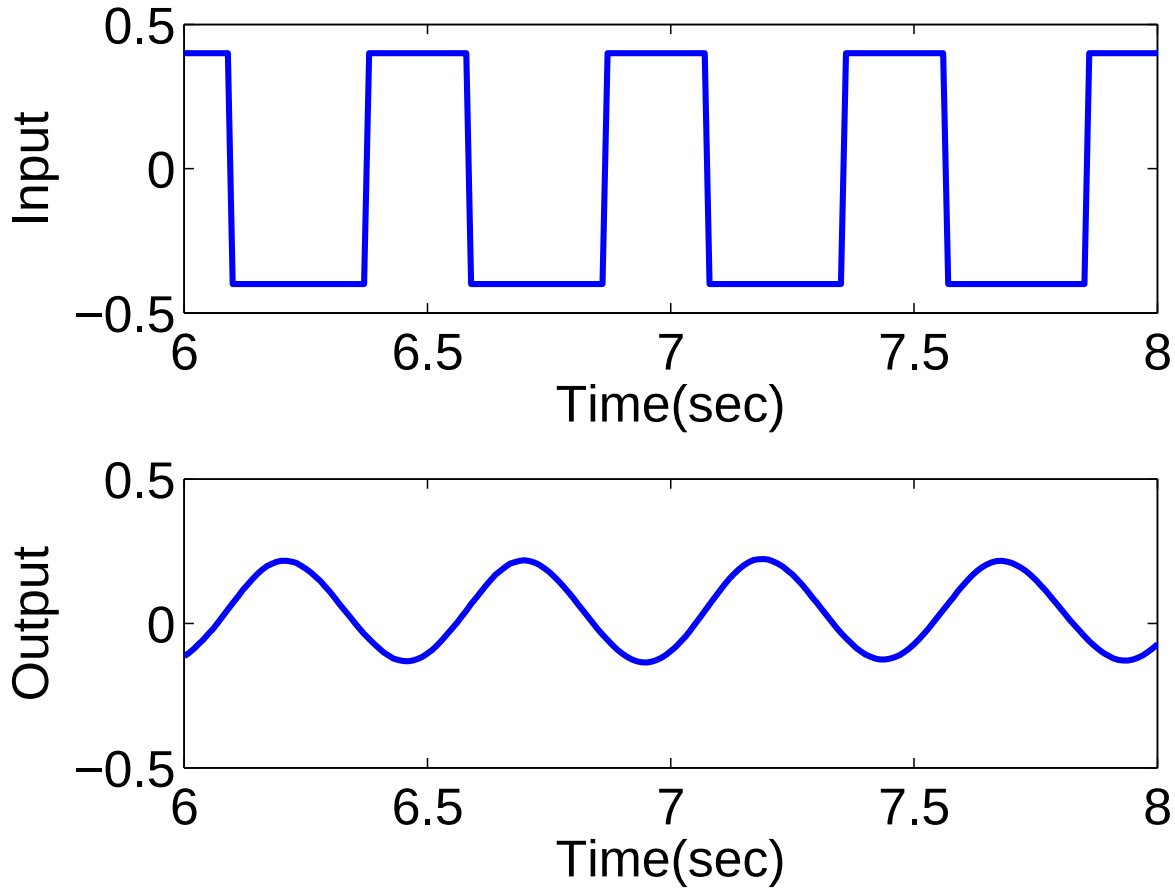

Figure 18: Relay feedback control signals from outer-loop system: top figure input signal; bottom figure output signal.

Closed-loop Control Results

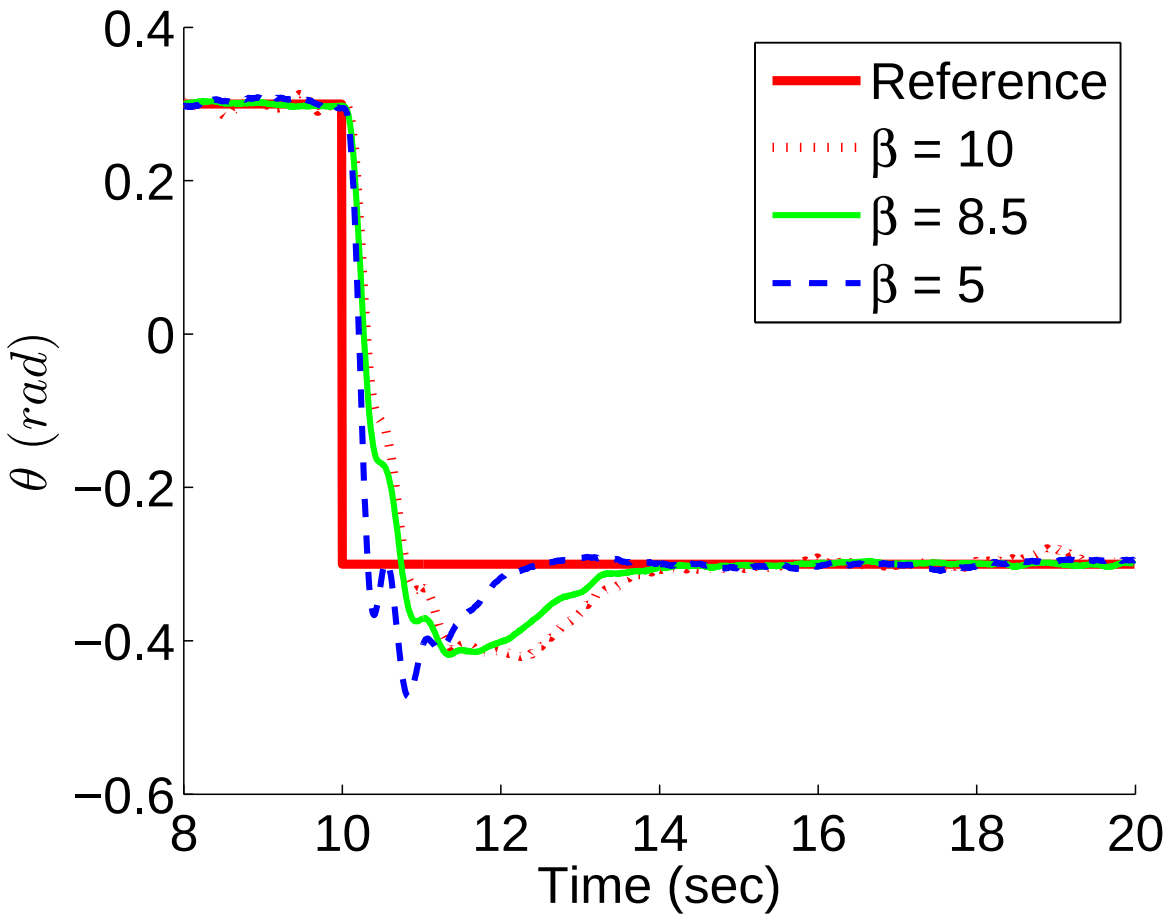

Figure 19: Comparative outer-loop step response in closed-loop control.

Application to Hexacopter

Table 4: Flight controller and avionic components

Components	Descriptions
Airframe	Turnigy Talon Hexacopter
Microprocessor	ATMega2560
Inertial measurement unit	MPU6050
Electronic speed controllers	Turnigy 25A Speed Controller
Brushless DC motors	NTM Prop Drive 28-26 235W
Propellers	10x4.5 SF Props
RC Receiver	OrangeRX R815X 2.4Ghz receiver
RC Transmitter	Turnigy 9XR PRO transmitter
Datalogger	CleanFlight Blackbox Datalogger

Relay experimental data

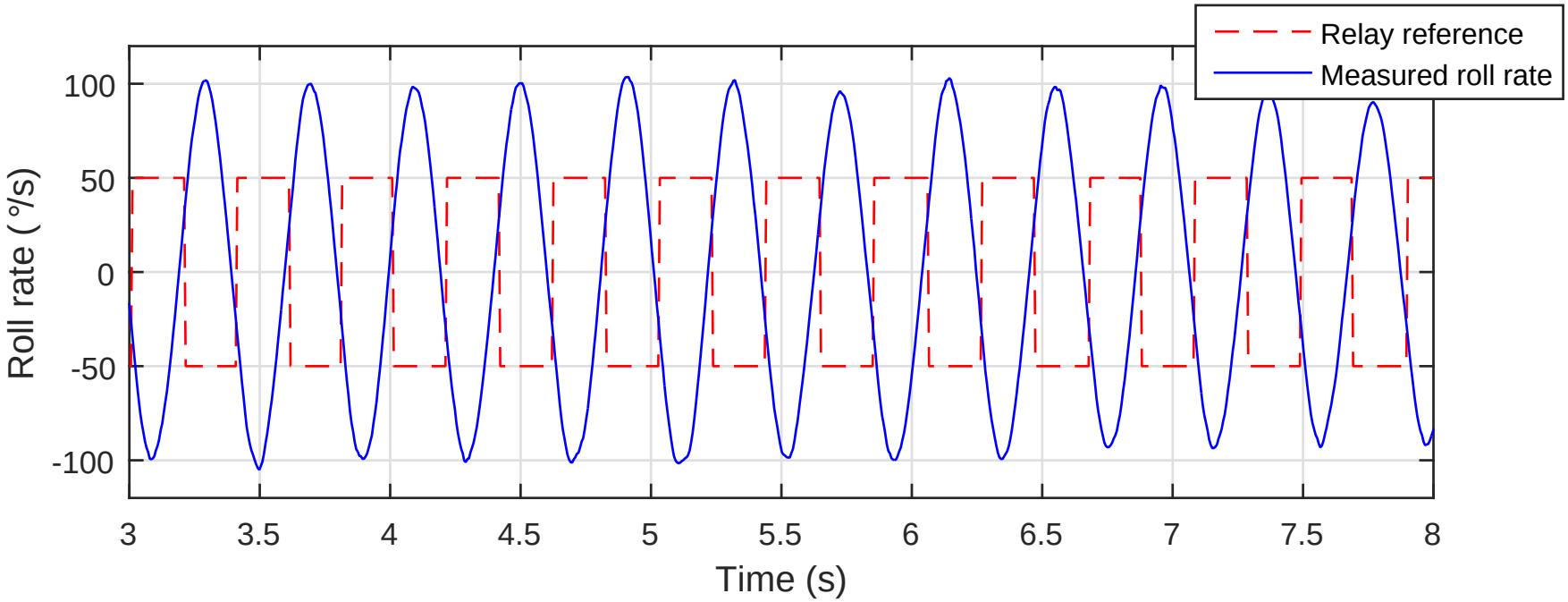

Figure 20: Inner loop relay test result. $K_T = 0.3$, $R_a = 50°/s$, $\epsilon = 30°/s$

Controller parameters

Controller parameters found for inner-loop

$K_c = 0.33, \tau_I = 0.26$ and $\tau_D = 0.03$

Controller parameters found for outer-loop

$K_c = 3.3$, $\tau_I = 0.63$ and $\tau_D = 0.013$.

Outdoor flight testing

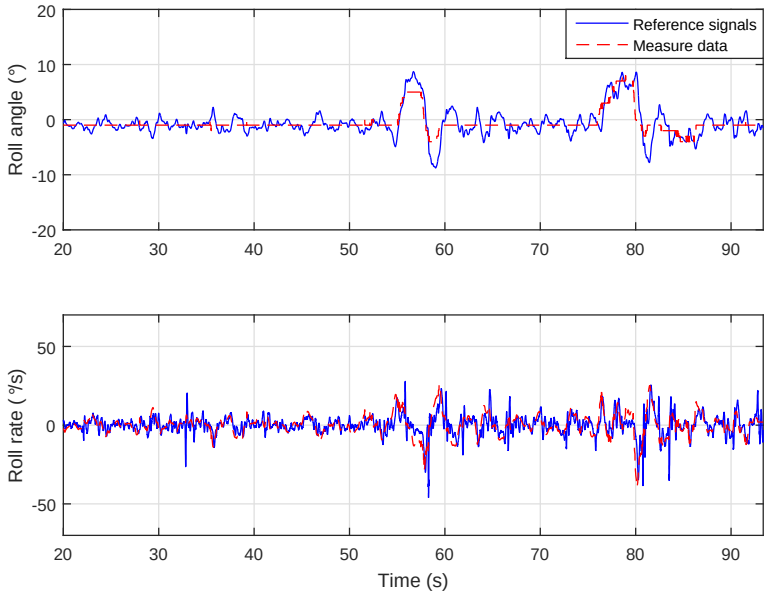

(a) Roll control:top-angle,bottom- rate

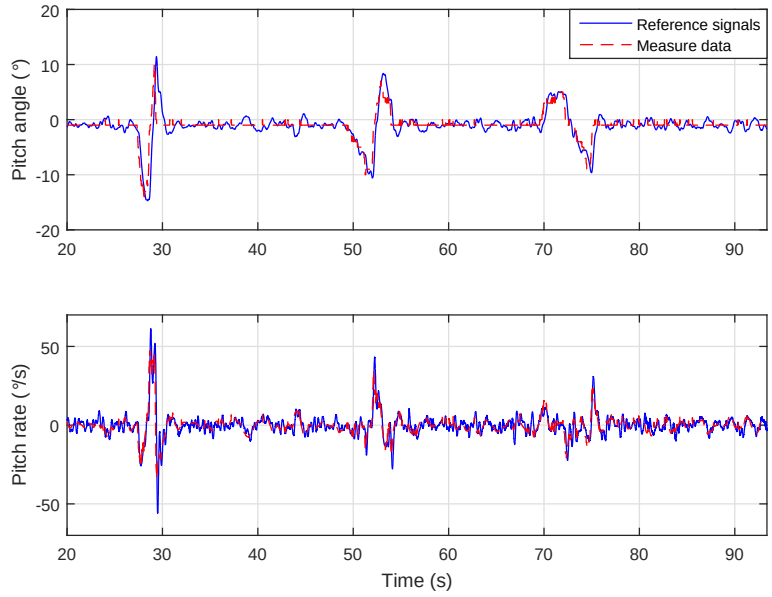

(b) Pitch control:top-angle,bottom- rate

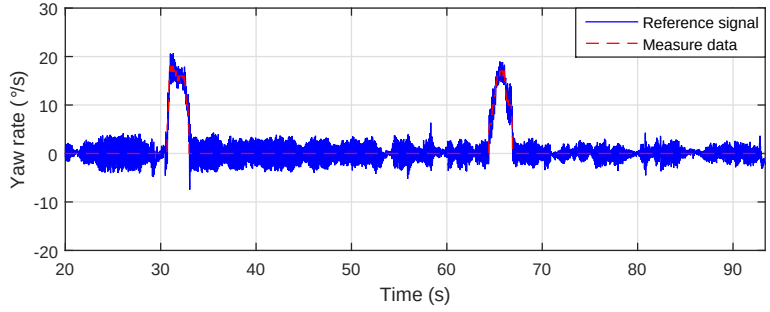

(c) Yaw control results

Figure 22: Experimental testing results. Key- red dashed lines: the reference signals; blue solid lines: the measured data

References

- Alfaro, V. M., Vilanova, R., 2016. Model-reference robust tuning of PID controllers. Springer.
- Astrom, K. J., Hagglund, T., 1988. Automatic Tuning of PID Controllers. Instrument Society of America, Research Triangle Park, NC.
- Astrom, K. J., Hagglund, T., 1995. PID Controllers:Theory, Design, and Tuning. Instrument Society of America, Research Triangle Park, NC.
- Astrom, K. J., Hagglund, T., 2006. Advanced PID control. Instrument Society of America, Research Triangle Park, NC.
- Visioli, A., 2006. Practical PID Control. Springer Science & Business Media.
- Wang, L., 2020. PID Control System Design and Automatic Tuning using MATLAB/Simulink. Wiley-IEEE PRESS.
- Wang, L., Chai, S., Yoo, D., Gan, L., Ng, K., 2015. PID and Predictive Control of Electrical Drives and Power Converters. Wiley-IEEE PRESS.